

Relaxation of Two-Spin Coherence Due to Cross-Correlated Fluctuations of Dipole–Dipole Couplings and Anisotropic Shifts in NMR of ^{15}N , ^{13}C -Labeled Biomolecules

Elisabetta Chiarparin,[†] Philippe Pelupessy,[†] Ranajeet Ghose,[†] and Geoffrey Bodenhausen^{*,†,‡}

Contribution from the Section de Chimie, Université de Lausanne, BCH, 1015 Lausanne, Switzerland, and Département de chimie, associé au CNRS, Ecole Normale Supérieure, 24 rue Lhomond, 75231 Paris Cedex 05, France

Received December 21, 1998. Revised Manuscript Received May 7, 1999

Abstract: A comprehensive description is presented of the effects on two-spin coherences (i.e., superpositions of zero- and double-quantum coherences) of cross-correlation between the fluctuations of two different relaxation mechanisms in nuclear magnetic resonance (NMR). Dipole–dipole (DD) interactions between four nuclei and chemical shift anisotropy (CSA) of two of these nuclei are considered. Two complementary experiments have been designed for ^{15}N , ^{13}C -labeled proteins to quantify the effects of cross-correlation between the $^{13}\text{C}^\alpha$ – $^1\text{H}^\alpha$ and ^{15}N – $^1\text{H}^\text{N}$ dipolar interactions on two-spin coherences involving $^{13}\text{C}^\alpha$ of the i th residue with the ^{15}N of the $(i+1)$ th amino acid. Two other experiments allow one to quantify the effect of cross-correlation between the $^{13}\text{C}'$ (carbonyl) CSA and the $^{13}\text{C}^\alpha$ – $^1\text{H}^\alpha$ dipolar coupling on the relaxation of two-spin coherences involving the $^{13}\text{C}'$ and $^{13}\text{C}^\alpha$ nuclei on the same residue of the protein. These experiments have been used to extract relevant cross-correlation rates in ^{15}N , ^{13}C -labeled human ubiquitin. These rates show a high degree of correlation with the backbone Ψ angles in proteins.

Introduction

In nuclear magnetic resonance (NMR), cross-correlation between the fluctuations of two different relaxation mechanisms has been shown to be a valuable source of information about structure^{1–3} and dynamics.^{4,5} Cross-correlation effects have also proven to be useful to study chemical exchange.⁶ After early seminal work by Wokaun and Ernst⁷ on the effects of correlated fluctuations of external fields on transverse relaxation of multiple quantum coherences, there has been a recent renewal of such studies.^{8–12} In particular, it is possible to quantify the effects of cross-correlation between the fluctuations of $^{13}\text{C}^\alpha$ – $^1\text{H}^\alpha$ and ^{15}N – $^1\text{H}^\text{N}$ dipolar couplings on the relaxation of two-spin coherences involving ^{15}N and $^{13}\text{C}^\alpha$ nuclei in a protein back-

bone.^{8,11,12} Similarly, cross-correlation between the chemical shift anisotropy (CSA) of a $^{13}\text{C}'$ (carbonyl) nucleus and a $^{13}\text{C}^\alpha$ – $^1\text{H}^\alpha$ dipolar coupling has been investigated.^{9,10,12} It has been shown that the corresponding relaxation rates allow one to determine backbone angles Ψ in proteins, which have been hitherto inaccessible. These experiments bear a relationship to methods designed to measure dihedral angles in the solid state.^{13,14}

This paper consists of three distinct parts. In the first part of the paper, we present a compact theory for the description of the effects on two-spin coherences (i.e., zero- and double-quantum coherences involving two spins) of correlated fluctuations of dipole–dipole and CSA interactions. In the second part, we present new experiments to measure these cross-correlation effects. Finally, in the third part, we relate two of the rates that we can measure accurately, namely the rate due to cross-correlation between $^{13}\text{C}^\alpha$ – $^1\text{H}^\alpha$ and ^{15}N – $^1\text{H}^\text{N}$ dipolar couplings and the rate due to the cross-correlation between the $^{13}\text{C}'$ CSA and the $^{13}\text{C}^\alpha$ – $^1\text{H}^\alpha$ dipolar coupling, to the backbone angles Ψ in human ubiquitin.

In a recent publication¹¹ we have described a method to measure the extent of cross-correlation of the fluctuations of ^{15}N – ^1H and $^{13}\text{C}^\alpha$ – $^1\text{H}^\alpha$ dipolar couplings, which affect the relaxation of two-spin coherences involving ^{15}N and $^{13}\text{C}^\alpha$. Cross-correlation leads to partial conversion of a density operator component $2\text{C}^\alpha_x\text{N}_x$ into $8\text{C}^\alpha_y\text{N}_y\text{H}^\alpha_z\text{H}^\text{N}_z$. This interconversion can be measured quantitatively by comparing signals obtained from two complementary two-dimensional experiments.^{11,15} In this

* To whom correspondence should be addressed. E-mail: Geoffrey.Bodenhausen@ens.fr. Phone: +33 1 44 32 34 0. Fax: +33 1 44 32 33 97.

[†] Université de Lausanne.

[‡] Ecole Normale Supérieure.

(1) Tjandra, N.; Szabo, A.; Bax, A. *J. Am. Chem. Soc.* **1996**, *118*, 6986.

Tjandra, N.; Bax, A. *J. Am. Chem. Soc.* **1997**, *119*, 8076.

(2) Konrat, R.; Sterk, H. *Chem. Phys. Lett.* **1993**, *203*, 75.

(3) Tessari, M.; Vis, H.; Boelens, R.; Kaptein, R.; Vuister, G. W. *J. Am. Chem. Soc.* **1997**, *119*, 8985.

(4) Fischer, M.; Zeng, L.; Pang, Y.; Hu, W.; Majumdar, A.; Zuiderweg, E. R. P. *J. Am. Chem. Soc.* **1997**, *119*, 12629.

(5) Yang, D.; Mittermaier, A.; Mok, Y. K.; Kay, L. E. *J. Mol. Biol.* **1998**, *276*, 939.

(6) Kroenke, C. D.; Loria, J. P.; Lee, L. K.; Rance, M.; Palmer, A., III. *J. Am. Chem. Soc.* **1998**, *120*, 7909.

(7) Wokaun, A.; Ernst, R. R. *Mol. Phys.* **1978**, *36*, 317.

(8) Reif, B.; Hennig, M.; Griesinger, C. *Science* **1997**, *276*, 1230.

(9) Yang, D.; Konrat, R.; Kay, L. E. *J. Am. Chem. Soc.* **1997**, *119*, 11938.

(10) Yang, D.; Gardner, K.; Kay, L. E. *J. Biomol. NMR* **1998**, *11*, 213.

(11) Pelupessy, P.; Chiarparin, E.; Ghose, R.; Bodenhausen, G. *J. Biomol. NMR* **1999**, *13*, 375.

(12) Yang, D.; Kay, L. E. *J. Am. Chem. Soc.* **1998**, *120*, 9880.

(13) Feng, X.; Lee, Y. K.; Sandström, D.; Edén, M.; Maisel, H.; Sebald, A.; Levitt, M. *Chem. Phys. Lett.* **1996**, *257*, 314.

(14) Schmidt-Rohr, K. *J. Am. Chem. Soc.* **1996**, *118*, 7601.

(15) Felli, I. C.; Richter, C.; Griesinger, C.; Schwalbe, H. *J. Am. Chem. Soc.* **1999**, *121*, 1956.

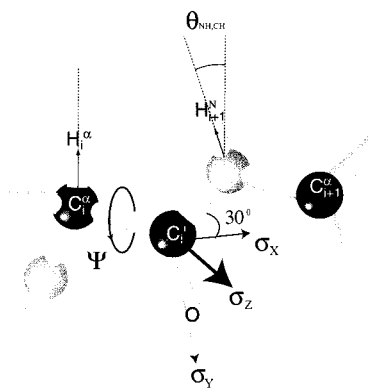


Figure 1. Nuclei belonging to the backbone of a protein that can sustain two-spin coherences which are affected by cross-correlation effects. The peptide plane is spanned by the five atoms C^α , C^β , O , N , and H^N . The CSA tensor of the carbonyl $^{13}C'$ nucleus has a principal component σ_y along the $C=O$ bond, a component σ_x that lies in the peptide plane, and a component σ_z that is perpendicular to this plane.

paper we extend the methodology to the measurement of cross-correlation between the $^{13}C'$ CSA and the $^{13}C^\alpha-^1H^\alpha$ dipolar coupling on the relaxation of two-spin coherences involving $^{13}C'$ and $^{13}C^\alpha$. The experiments described in our earlier publication involved a fixed relaxation delay T , which had to be chosen to be a multiple of the inverse of the scalar coupling $^1J(C^\alpha C^\beta)$ (~ 35 Hz), to minimize losses of coherence. Such long delays (on the order of 25 ms) are unfavorable in large proteins with short transverse relaxation times. In the experiments described here, in analogy to experiments described by Yang et al.,¹⁰ we have used band-selective pulses applied to $^{13}C^\alpha$ (but not to $^{13}C'$ and $^{13}C^\beta$), so that one can choose relaxation delays of arbitrary duration T .

Theory

In this section, we shall consider cross-correlation effects involving various nuclei in the peptide plane shown in Figure 1.

$C^\alpha H^\alpha/NH^N$ Dipole–Dipole Cross-Correlation. Consider an initial density operator consisting of a suitably excited two-spin coherence, i.e., $\sigma(0) = 2C^\alpha_x N_x$. The main interactions that need to be taken into account to describe the transverse relaxation of this term are the two chemical shift anisotropies $CSA\{^{13}C^\alpha\}$ and $CSA\{^{15}N\}$, and the four dipolar couplings $DD\{^{13}C^\alpha-^1H^\alpha\}$, $DD\{^{13}C^\alpha-^1H^N\}$, $DD\{^{15}N-^1H^N\}$ and $DD\{^{15}N-^1H^\alpha\}$. The relevant cross-correlated relaxation mechanisms are summarized in Table 1 and represented graphically in Figure 2. If the rotational diffusion is in the slow-tumbling regime, only the zero-frequency components of the spectral density functions, i.e., the $J(0)$ terms (see the Appendix, section B) can make significant contributions to the relaxation rates. The density operator, $\sigma(t)$, can be expanded in a suitable basis of orthogonal operators $\{B_k\}$:¹⁶

$$\sigma(t) = \sum_k b_k(t) B_k \quad (1)$$

where the time dependence is contained in the coefficients $b_k(t)$. The spin dynamics are governed by the master equation, which can be represented in matrix form as

$$d\mathbf{b}/dt = -\mathbf{R}\mathbf{b} \quad (2)$$

(16) Ernst, R. R.; Bodenhausen, G.; Wokaun, A. *Principles of Nuclear Magnetic Resonance in One and Two Dimensions*; Clarendon Press: Oxford, 1987.

Table 1. Cross-Correlated Interactions in a $^1H^\alpha-^{13}C^\alpha-...-^{15}N-^1H^N$ System^{a,b}

	$R_{DQ\alpha\alpha}$	$R_{DQ\alpha\beta}$	$R_{DQ\beta\alpha}$	$R_{DQ\beta\beta}$	$R_{ZQ\alpha\alpha}$	$R_{ZQ\alpha\beta}$	$R_{ZQ\beta\alpha}$	$R_{ZQ\beta\beta}$
$R_{C^\alpha H^\alpha, NH^N}$	+	-	-	+	-	+	+	-
$R_{C^\alpha H^N, NH^\alpha}$	+	-	-	+	-	+	+	-
$R_{C^\alpha H^\alpha, C^\alpha H^\alpha}$	+	-	-	+	+	-	-	+
R_{NH^α, NH^N}	+	-	-	+	+	-	-	+
$R_{C^\alpha H^\alpha, NH^\alpha}$	+	+	+	+	-	-	-	-
$R_{C^\alpha, N}$	+	+	+	+	-	-	-	-
$R_{C^\alpha H^N, NH^N}$	+	+	+	+	-	-	-	-
$R_{C^\alpha, C^\alpha H^\alpha}$	+	+	-	-	+	+	-	-
R_{N, NH^α}	+	+	-	-	+	+	-	-
$R_{N, C^\alpha H^\alpha}$	+	+	-	-	-	-	+	+
R_{C^α, NH^α}	+	+	-	-	-	-	+	+
R_{C^α, NH^N}	+	-	+	-	-	+	-	+
$R_{N, C^\alpha H^N}$	+	-	+	-	-	+	-	+
$R_{C^\alpha, C^\alpha H^N}$	+	-	+	-	+	-	+	-
R_{N, NH^N}	+	-	+	-	+	-	+	-

^a The + and - signs in the table indicate whether the contribution of a particular term must be added to or subtracted from the average transverse relaxation rates. ^b See the Appendix, section B, for explicit expressions of the rates.

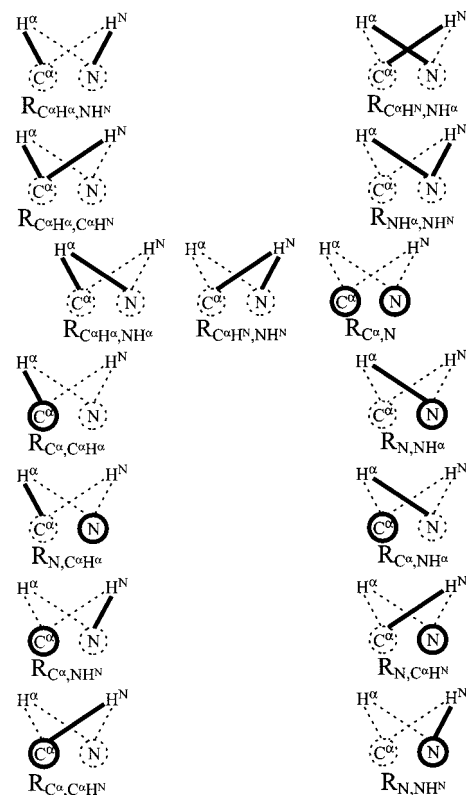


Figure 2. Pictograms representing various interactions in a $^1H^\alpha-^{13}C^\alpha-...-^{15}N-^1H^N$ subsystem. Bold lines and circles stand for the DD and CSA interactions that are responsible for various cross-correlated relaxation effects. Pictograms shown on the same row produce analogous effects on the relaxation of two-spin coherence $2C^\alpha_x N_x$.

where the coefficients $b_k(t)$ are collected into a vector \mathbf{b} . The matrix \mathbf{R} describes both relaxation and coherent evolution. Each coherence associated with a pair of eigenstates, i.e., with a single transition, can be represented by a product of shift operators I_+ and I_- (which will be denoted $C^{\alpha+}$, $C^{\alpha-}$, N_+ , and N_- to indicate the chemical identity of the spins that carry the angular momentum) and polarization operators $I_\alpha = E/2 + I_z$ and $I_\beta = E/2 - I_z$, where E represents the identity operator.¹⁶ These will likewise be denoted H^α_α , H^α_β , H^N_α , and H^N_β . Thus, the four lines of the doublet-of-doublets in the double-quantum spectrum associated with the coherence $C^{\alpha+}N_+$ can be associated with the four single-transition operators $C^{\alpha+}N_+H^\alpha_\alpha H^N_\alpha$,

$C^{\alpha}_+N_+H^{\alpha}_\alpha H^N_\beta$, $C^{\alpha}_+N_+H^{\alpha}_\beta H^N_\alpha$, and $C^{\alpha}_+N_+H^{\alpha}_\beta H^N_\beta$. A similar notation may be used for the coherences of order $p = 0$ and -2 . The relaxation matrix \mathbf{R} has a block diagonal form consisting of four 4-dimensional subspaces spanned by subsets of basis functions. Thus, the $p = +2$ and one of the $p = 0$ manifolds may be written as

$$\mathbf{b}^{++} = \begin{pmatrix} \langle 2C^{\alpha}_+N_+H^{\alpha}_\alpha H^N_\alpha \rangle \\ \langle 2C^{\alpha}_+N_+H^{\alpha}_\alpha H^N_\beta \rangle \\ \langle 2C^{\alpha}_+N_+H^{\alpha}_\beta H^N_\alpha \rangle \\ \langle 2C^{\alpha}_+N_+H^{\alpha}_\beta H^N_\beta \rangle \end{pmatrix} \quad \mathbf{b}^{+-} = \begin{pmatrix} \langle 2C^{\alpha}_+N_-H^{\alpha}_\alpha H^N_\alpha \rangle \\ \langle 2C^{\alpha}_+N_-H^{\alpha}_\alpha H^N_\beta \rangle \\ \langle 2C^{\alpha}_+N_-H^{\alpha}_\beta H^N_\alpha \rangle \\ \langle 2C^{\alpha}_+N_-H^{\alpha}_\beta H^N_\beta \rangle \end{pmatrix} \quad (3)$$

The elements of the vectors \mathbf{b}^{+-} and \mathbf{b}^{++} transform as complex conjugates of \mathbf{b}^{+-} and \mathbf{b}^{++} , respectively. Therefore, it is sufficient to follow the evolution of the former two vectors explicitly. The basis functions have the same norm as the Cartesian operators. The evolution of \mathbf{b}^{++} and \mathbf{b}^{+-} in their respective subspaces is described by

$$d\mathbf{b}^{++}/dt = -\mathbf{R}^{++}\mathbf{b}^{++} \quad (4a)$$

$$d\mathbf{b}^{+-}/dt = -\mathbf{R}^{+-}\mathbf{b}^{+-} \quad (4b)$$

where \mathbf{R}^{++} and \mathbf{R}^{+-} are given by

$$\mathbf{R}^{++} = \begin{pmatrix} i\pi J_{++} + R_{av} + R_{DQ\alpha\alpha} & \frac{R_{ii} + R_{ai} - R_{ia} - R_{aa}}{4} & \frac{R_{ii} - R_{ai} + R_{ia} - R_{aa}}{4} & \frac{R_{ii} - R_{ai} - R_{ia} + R_{aa}}{4} \\ \frac{R_{ii} + R_{ai} - R_{ia} - R_{aa}}{4} & i\pi J_{+-} + R_{av} + R_{DQ\alpha\beta} & \frac{R_{ii} - R_{ai} - R_{ia} + R_{aa}}{4} & \frac{R_{ii} - R_{ai} + R_{ia} - R_{aa}}{4} \\ \frac{R_{ii} - R_{ai} + R_{ia} - R_{aa}}{4} & \frac{R_{ii} - R_{ai} - R_{ia} + R_{aa}}{4} & -i\pi J_{+-} + R_{av} + R_{DQ\beta\alpha} & \frac{R_{ii} + R_{ai} - R_{ia} - R_{aa}}{4} \\ \frac{R_{ii} - R_{ai} - R_{ia} + R_{aa}}{4} & \frac{R_{ii} - R_{ai} + R_{ia} - R_{aa}}{4} & \frac{R_{ii} + R_{ai} - R_{ia} - R_{aa}}{4} & -i\pi J_{++} + R_{av} + R_{DQ\beta\beta} \end{pmatrix} \quad (5a)$$

$$\mathbf{R}^{+-} = \begin{pmatrix} i\pi J_{+-} + R_{av} + R_{ZQ\alpha\alpha} & \frac{R_{ii} + R_{ai} - R_{ia} - R_{aa}}{4} & \frac{R_{ii} - R_{ai} + R_{ia} - R_{aa}}{4} & \frac{R_{ii} - R_{ai} - R_{ia} + R_{aa}}{4} \\ \frac{R_{ii} + R_{ai} - R_{ia} - R_{aa}}{4} & i\pi J_{++} + R_{av} + R_{ZQ\alpha\beta} & \frac{R_{ii} - R_{ai} - R_{ia} + R_{aa}}{4} & \frac{R_{ii} - R_{ai} + R_{ia} - R_{aa}}{4} \\ \frac{R_{ii} - R_{ai} + R_{ia} - R_{aa}}{4} & \frac{R_{ii} - R_{ai} - R_{ia} + R_{aa}}{4} & -i\pi J_{++} + R_{av} + R_{ZQ\beta\alpha} & \frac{R_{ii} + R_{ai} - R_{ia} - R_{aa}}{4} \\ \frac{R_{ii} - R_{ai} - R_{ia} + R_{aa}}{4} & \frac{R_{ii} - R_{ai} + R_{ia} - R_{aa}}{4} & \frac{R_{ii} + R_{ai} - R_{ia} - R_{aa}}{4} & -i\pi J_{+-} + R_{av} + R_{ZQ\beta\beta} \end{pmatrix} \quad (5b)$$

with the effective scalar couplings

$$\begin{aligned} J_{++} &= {}^1J(C^{\alpha}H^{\alpha}) + {}^1J(NH^N) \\ J_{+-} &= {}^1J(C^{\alpha}H^{\alpha}) - {}^1J(NH^N) \end{aligned} \quad (6)$$

Since chemical shifts are refocused in our experiments, they need not be considered in eq 5. The average rate appearing in the diagonal terms is $R_{av} = (R_{ii} + R_{ia} + R_{ai} + R_{aa})/4$. The rates R_{ii} , R_{ia} , R_{ai} , and R_{aa} are the autorelaxation rates of the in-phase and antiphase terms $2C^{\alpha}_xN_x$, $4C^{\alpha}_xN_xH^N_z$, $4C^{\alpha}_xN_xH^{\alpha}_z$, and $8C^{\alpha}_xN_xH^N_zH^{\alpha}_z$, respectively. For the time being, we assume that these relaxation rates are equal for the zero- and double-quantum manifolds. The other contributions to the diagonal elements of the matrixes of eq 5 are due to cross-correlation between the different interactions mentioned before. Each of these rates comprises up to 15 rates that are due to different cross-correlated relaxation mechanisms (see Table 1 and Figure 2 for further details). It is convenient to study the effects of the off-diagonal elements on the spin dynamics using perturbation theory¹⁸ (Appendix, section A). One can safely neglect the off-diagonal

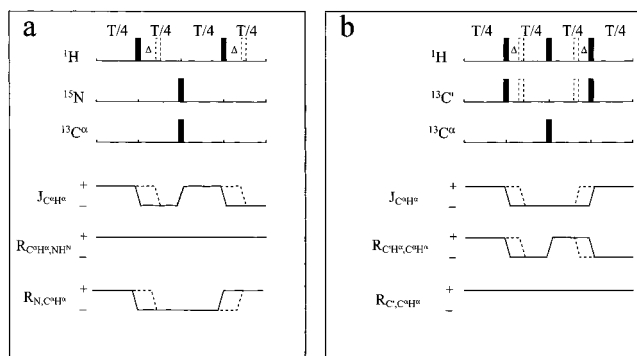


Figure 3. Manipulations by sequences of π pulses of two-spin coherences (a) $2C^{\alpha}_xN_x$ and (b) $2C^{\alpha}_x C^{\alpha}_x$. These schemes are designed to measure the cross-correlated rates $R_{C^{\alpha}H^{\alpha},NH^{\alpha}}$ and $R_{C^{\alpha}H^{\alpha},C^{\alpha}}$, respectively. If the pulses are positioned as shown by filled symbols, evolution under chemical shifts of the heteronuclei and scalar couplings $J(NH)$ and $J(CH)$ are suppressed. In (a) all DD-CSA cross-correlation effects are removed because the proton π pulses invert both H^{α} and H^N . If these two pulses are shifted simultaneously in the same direction, this does not affect any of the cross-correlation rates of Table 1, while evolution under scalar couplings $J(C^{\alpha}H^{\alpha})$ and $J(NH^N)$ is no longer canceled. The toggling frame pictures below show how the scalar couplings and cross-relaxation rates change sign as a result of applying π pulses. In (a) $J(NH^N)$ transforms in the same manner as $J(C^{\alpha}H^{\alpha})$. The rates in Tables 1 and 2 behave as follows: with reference to (a) rates 1–7 of Table 1 as $R_{C^{\alpha}H^{\alpha},NH^{\alpha}}$ and rates 8–15 of Table 1 as $R_{N,C^{\alpha}H^{\alpha}}$; with reference to (b) rates 1 and 2 of Table 2 as $R_{C^{\alpha}H^{\alpha},C^{\alpha}}$ and rates 3–6 of Table 2 as $R_{C^{\alpha}H^{\alpha},C^{\alpha}}$. In (b) only the effects of the rates $R_{C^{\alpha}H^{\alpha},C^{\alpha}}$ and $R_{C^{\alpha}H^{\alpha},C^{\alpha}}$ are retained. If the outer 1H and ${}^{13}C'$ pulses are simultaneously moved toward the center, the overall effect of the cross-correlation rates of Table 2 is not modified, while scalar coupling evolution can occur. Note that the chemical shift of the carbonyl is not refocused anymore.

elements provided that $|R_{aa} - R_{ai}|$, $|R_{ia} - R_{ii}|$, $|R_{aa} - R_{ia}|$, $|R_{ai} - R_{ii}| \ll |4\pi^1J(C^{\alpha}H^{\alpha})| - |4\pi^1J(NH^N)|$. In this case, only the diagonal elements R_{kk} of the \mathbf{R} matrix need to be considered, so that all coherences feature monoexponential decays:

$$b_k(t) = b_k(0) \exp(-R_{kk}t) \quad (7)$$

The effect of π pulses on the ${}^{13}C^{\alpha}$, ${}^{15}N$, and 1H channels is to interchange C^{α}_+ with C^{α}_- , N_+ with N_- , and H_{α} with H_{β} , respectively. If one or more π pulses are applied between consecutive time intervals of duration Δt_n , the various operators B_k will be interconverted. After the last interval at $T = \sum \Delta t_n$ the components of \mathbf{b} are

$$b_i(T) = b_j(0) \prod_{n=1}^N \exp(-R_{kk}\Delta t_n) \quad (8)$$

where the density operator is in the state B_j at the beginning, B_k in the n th interval Δt_n , and B_i at time T .

The scheme in Figure 3a has been designed to measure the cross-correlated relaxation between the dipolar interactions ${}^{13}C^{\alpha}-{}^1H^{\alpha}$ and ${}^{15}N-{}^1H^N$. In the slow tumbling limit, the only fluctuating dipolar Hamiltonians that contribute to this relaxation mechanism are proportional to $C^{\alpha}_zH^{\alpha}_z$ and $N_zH^N_z$. The effect of dipole–dipole cross-correlation on the initial density operator $\sigma(0) = 2C^{\alpha}_xN_x$ is a partial conversion into a term $\sigma(T) = 8C^{\alpha}_yN_yH^{\alpha}_zH^N_z$. It is important that the pulses interconvert the coherences in such a way that the sign of the rate $R_{C^{\alpha}H^{\alpha},NH^{\alpha}}$

(17) Brutscher, B.; Bremi, T.; Skrynnikov, N.; Brüschweiler, R.; Ernst, R. R. *J. Magn. Reson.* **1998**, *130*, 346.

(18) Merzbacher, E. *Quantum Mechanics*, 2nd ed.; Wiley: New York, 1970.

that one wishes to measure is preserved (see Table 1 and toggling frame diagrams in Figure 3a). This can be achieved by applying π pulses simultaneously to two of the four nuclei involved. Thus in Figure 3a two ^1H π pulses are applied at $T/4$ and at $3T/4$, while π pulses are applied at $T/2$ simultaneously to the ^{13}C and ^{15}N channels. The ^1H pulses average out the CSA–dipole interactions (the last eight terms in Table 1), while ^{13}C and ^{15}N pulses refocus the chemical shift evolution. Using eq 8 one can calculate the density operator at time T and, therefore, the expectation values of the operators of interest:

$$\begin{aligned} \langle 2C_x^\alpha N_x \rangle &= 1/4(\langle 2C_{+N}^\alpha H_\alpha^\alpha H_\alpha^N \rangle + \langle 2C_{+N}^\alpha H_\alpha^\alpha H_\beta^N \rangle + \\ &\quad \langle 2C_{+N}^\alpha H_\beta^\alpha H_\alpha^N \rangle + \langle 2C_{+N}^\alpha H_\beta^\alpha H_\beta^N \rangle + \\ &\quad \langle 2C_{+N}^\alpha H_\alpha^\alpha H_\alpha^N \rangle + \langle 2C_{+N}^\alpha H_\alpha^\alpha H_\beta^N \rangle + \\ &\quad \langle 2C_{+N}^\alpha H_\beta^\alpha H_\alpha^N \rangle + \langle 2C_{+N}^\alpha H_\beta^\alpha H_\beta^N \rangle + \text{cc}) \\ &= 1/4\{\exp[(\Gamma_2 + \Gamma_3)T] + \exp[-(\Gamma_2 + \Gamma_3)T]\} \\ &\quad \exp[-(R_{\text{av}} + \Gamma_1)T] + 1/4\{(\Gamma_2 - \Gamma_3)T\} + \\ &\quad \exp[-(\Gamma_2 - \Gamma_3)T] \exp[-(R_{\text{av}} + \Gamma_1)T] \quad (9a) \end{aligned}$$

$$\begin{aligned} \langle 8C_y^\alpha N_y H_z^\alpha H_z^N \rangle &= 1/4(-\langle 2C_{+N}^\alpha H_\alpha^\alpha H_\alpha^N \rangle + \\ &\quad \langle 2C_{+N}^\alpha H_\alpha^\alpha H_\beta^N \rangle + \langle 2C_{+N}^\alpha H_\beta^\alpha H_\alpha^N \rangle - \\ &\quad \langle 2C_{+N}^\alpha H_\beta^\alpha H_\beta^N \rangle + \langle 2C_{+N}^\alpha H_\alpha^\alpha H_\alpha^N \rangle - \\ &\quad \langle 2C_{+N}^\alpha H_\alpha^\alpha H_\beta^N \rangle - \langle 2C_{+N}^\alpha H_\beta^\alpha H_\alpha^N \rangle + \\ &\quad \langle 2C_{+N}^\alpha H_\beta^\alpha H_\beta^N \rangle + \text{cc}) \\ &= -1/4\{\exp[(\Gamma_2 + \Gamma_3)T] + \\ &\quad \exp[-(\Gamma_2 + \Gamma_3)T]\} \exp[-(R_{\text{av}} + \Gamma_1)T] + \\ &\quad 1/4\{\exp[(\Gamma_2 - \Gamma_3)T] + \\ &\quad \exp[-(\Gamma_2 - \Gamma_3)T]\} \exp[-(R_{\text{av}} - \Gamma_1)T] \quad (9b) \end{aligned}$$

where cc stands for complex conjugate, and where

$$\Gamma_1 = R_{C^\alpha H^\alpha, N^{\text{HN}}} + R_{C^\alpha H^\alpha, N^{\text{H}^\alpha}} \quad (10a)$$

$$\Gamma_2 = R_{C^\alpha H^\alpha, C^\alpha H^\alpha} + R_{N^{\text{H}^\alpha}, N^{\text{HN}}} \quad (10b)$$

$$\Gamma_3 = R_{C^\alpha H^\alpha, N^{\text{H}^\alpha}} + R_{C^\alpha, N} + R_{C^\alpha H^\alpha, N^{\text{HN}}} \quad (10c)$$

Provided $\Gamma_2 T \ll 1$ and $\Gamma_3 T \ll 1$, the ratio of the two expectation values is given by

$$\frac{\langle 8C_y^\alpha N_y H_z^\alpha H_z^N \rangle}{\langle 2C_x^\alpha N_x \rangle} = \tanh(\Gamma_1 T) \quad (11a)$$

We shall see that this ratio can be determined from the ratio of the cross-peak intensities of two complementary experiments labeled I and II:

$$a(\text{II})/a(\text{I}) = -\tanh(\Gamma_1 T) \quad (11b)$$

$C^\alpha H^\alpha/C'$ Dipole–CSA Cross-Correlation. The dipole–CSA cross-correlated relaxation of the multiple quantum manifold $C'_x C_x^\alpha$ can be treated in a similar fashion.¹⁷ The relevant mechanisms involved are CSA $\{^{13}\text{C}^\alpha\}$ and CSA $\{^{13}\text{C}'\}$ and the dipolar couplings DD $\{^{13}\text{C}^\alpha-^1\text{H}^\alpha\}$ and DD $\{^{13}\text{C}'-^1\text{H}^\alpha\}$. When the single transition operators are chosen as a basis, the relaxation matrix is reduced to four 2×2 blocks. For the $p = +2$ and one of the $p = 0$ blocks, the components of vector \mathbf{b} , in analogy to eq 3, are given by

$$\mathbf{b}^{++} = \begin{pmatrix} \langle \sqrt{2}C_{+C'}^\alpha C'_+ H_\alpha^\alpha \rangle \\ \langle \sqrt{2}C_{+C'}^\alpha C'_+ H_\beta^\alpha \rangle \end{pmatrix} \quad \mathbf{b}^{+-} = \begin{pmatrix} \langle \sqrt{2}C_{+C'}^\alpha C'_+ H_\alpha^\alpha \rangle \\ \langle \sqrt{2}C_{+C'}^\alpha C'_+ H_\beta^\alpha \rangle \end{pmatrix} \quad (12)$$

The vectors \mathbf{b}^{--} and \mathbf{b}^{-+} transform as complex conjugates of \mathbf{b}^{++} and \mathbf{b}^{+-} , respectively. The evolution of \mathbf{b}^{++} and \mathbf{b}^{+-} in their subspaces is described by eq 4 with

$$\mathbf{R}^{++} = \begin{pmatrix} i\pi J(C^\alpha H^\alpha) + R_{\text{av}} + R_{\text{DQ}\alpha} \frac{R_i - R_a}{2} \\ \frac{R_i - R_a}{2} \end{pmatrix} \begin{pmatrix} \frac{R_i - R_a}{2} \\ -i\pi J(C^\alpha H^\alpha) + R_{\text{av}} + R_{\text{DQ}\beta} \end{pmatrix} \quad (13a)$$

$$\mathbf{R}^{+-} = \begin{pmatrix} i\pi J(C^\alpha H^\alpha) + R_{\text{av}} + R_{\text{ZQ}\alpha} \frac{R_i - R_a}{2} \\ \frac{R_i - R_a}{2} \end{pmatrix} \begin{pmatrix} \frac{R_i - R_a}{2} \\ -i\pi J(C^\alpha H^\alpha) + R_{\text{av}} + R_{\text{ZQ}\beta} \end{pmatrix} \quad (13b)$$

where R_i and R_a indicate the auto-relaxation rates of the in-phase and antiphase terms $2C_x^\alpha C'_x$ and $4C_x^\alpha C'_x H_z^\alpha$. R_{av} is the average of R_i and R_a . The remaining rates in the diagonal elements are due to cross-correlation between the four relevant mechanisms (see Table 2). If $|R_i - R_a| \ll |4\pi J(C^\alpha H^\alpha)|$, the off-diagonal terms can be neglected.¹⁷

The cross-correlated relaxation between CSA $\{^{13}\text{C}'\}$ and DD $\{^{13}\text{C}^\alpha-^1\text{H}^\alpha\}$ leads to a partial conversion of $2C_x^\alpha C'_x$ into $4C_y^\alpha C'_y H_z^\alpha$ and can be measured with the scheme proposed in Figure 3b. It is necessary to invert two of the three nuclei involved in order to maintain the relative signs of the cross-correlation rate that one wishes to determine. At $T/4$ and $3T/4$, ^1H and $^{13}\text{C}'$ π pulses are applied simultaneously, while at $T/2$ ^1H and $^{13}\text{C}^\alpha$ π pulses are applied. The overall effect is to retain only the CSA–dipole interactions involving three different nuclei (the first two terms in Table 2) and to refocus the chemical shift evolution. Using eq 8, one can calculate the expectation values of the relevant operators:

$$\begin{aligned} \langle 2C_x^\alpha C'_x \rangle &= (\sqrt{2}/4)(\langle \sqrt{2}C_{+C'}^\alpha C'_+ H_\alpha^\alpha \rangle + \langle \sqrt{2}C_{+C'}^\alpha C'_+ H_\beta^\alpha \rangle + \\ &\quad \langle \sqrt{2}C_{+C'}^\alpha C'_+ H_\alpha^\alpha \rangle + \langle \sqrt{2}C_{+C'}^\alpha C'_+ H_\beta^\alpha \rangle + \text{cc}) \\ &= 1/2(\exp[-(R_{\text{av}} - \Gamma_1)T] + \exp[-(R_{\text{av}} + \Gamma_1)T]) \quad (14a) \end{aligned}$$

$$\begin{aligned} \langle 4C_y^\alpha C'_y H_z^\alpha \rangle &= (\sqrt{2}/4)(\langle -\sqrt{2}C_{+C'}^\alpha C'_+ H_\alpha^\alpha \rangle + \\ &\quad \langle \sqrt{2}C_{+C'}^\alpha C'_+ H_\beta^\alpha \rangle + \langle \sqrt{2}C_{+C'}^\alpha C'_+ H_\alpha^\alpha \rangle - \langle \sqrt{2}C_{+C'}^\alpha C'_+ H_\beta^\alpha \rangle + \\ &\quad \text{cc}) = 1/2(\exp[-(R_{\text{av}} - \Gamma_1)T] + \exp[-(R_{\text{av}} + \Gamma_1)T]) \quad (14b) \end{aligned}$$

where

$$\Gamma_1' = R_{C', C^\alpha H^\alpha} + R_{C', C^\alpha} \quad (15)$$

The ratio of the two expectation values is

$$\frac{\langle 4C_y^\alpha C'_y H_z^\alpha \rangle}{\langle 2C_x^\alpha C'_x \rangle} = \tanh(\Gamma_1' T) \quad (16a)$$

We shall see that this ratio can be determined from the ratio of the cross-peak intensities of two complementary experiments labeled I' and II':

Table 2. Cross-Correlated Interactions in a $^{13}\text{C}'-^{13}\text{C}^\alpha-^1\text{H}^\alpha$ System^{a,b}

	$R_{\text{DQ}\alpha}$	$R_{\text{DQ}\beta}$	$R_{\text{ZQ}\alpha}$	$R_{\text{ZQ}\beta}$
$R_{\text{C}'\text{C}^\alpha\text{H}^\alpha}$	+	-	-	+
$R_{\text{C}^\alpha\text{C}'\text{H}^\alpha}$	+	-	-	+
$R_{\text{C}'\text{H}^\alpha\text{C}^\alpha\text{H}^\alpha}$	+	+	-	-
$R_{\text{C}'\text{C}^\alpha}$	+	+	-	-
$R_{\text{C}^\alpha\text{C}'\text{H}^\alpha}$	+	-	+	-
$R_{\text{C}'\text{C}'\text{H}^\alpha}$	+	-	+	-

^a The + and - signs in the table indicate whether the contribution of a particular term must be added to or subtracted from the average transverse relaxation rates. ^b See the Appendix, section B, for explicit expressions of the rates.

$$a(\text{II}')/a(\text{I}') = \tanh(\Gamma_1' T) \quad (16\text{b})$$

Other Effects. So far it has been assumed that the double- and zero-quantum operators have the same average self-relaxation behavior. In a more rigorous treatment, the average rates R_{av} in eqs 5 and 13 have to be replaced by $R_{\text{av}}^{\text{DQ}}$ and $R_{\text{av}}^{\text{ZQ}}$ in the double- and zero-quantum subspaces, respectively. We can define a new average, $R'_{\text{av}} = 1/2(R_{\text{av}}^{\text{DQ}} + R_{\text{av}}^{\text{ZQ}})$ so that $R_{\text{av}}^{\text{DQ}} = R'_{\text{av}} + \delta$ and $R_{\text{av}}^{\text{ZQ}} = R'_{\text{av}} - \delta$, with $\delta = 1/2(R_{\text{av}}^{\text{DQ}} - R_{\text{av}}^{\text{ZQ}})$. The term δ has an effect similar to that due to the CSA-CSA cross-correlated relaxation mechanism, so that we can include it in the corresponding rates by substituting $R_{\text{C}\alpha,\text{N}} \Rightarrow R_{\text{C}\alpha,\text{N}} + \delta$ and $R_{\text{C}\alpha,\text{C}'} \Rightarrow R_{\text{C}\alpha,\text{C}'} + \delta$. Further cross-correlated rates of interactions involving remote nuclei can be included in the autorelaxation rate.

Measurement of the Backbone Angle Ψ . In proteins, the relaxation rates Γ_1 and Γ_1' defined above are related to the backbone angle Ψ . Since $R_{\text{C}'\text{H}^\alpha\text{NH}^\text{N}} \gg R_{\text{C}^\alpha\text{H}^\alpha\text{NH}^\text{N}}$, one obtains $\Gamma_1 \approx R_{\text{C}'\text{H}^\alpha\text{NH}^\text{N}}$, because of the unequal internuclear distances, and one may write in the slow-tumbling limit

$$\Gamma_1 = \left(\frac{\mu_0 \hbar}{4\pi}\right)^2 \frac{\gamma_{\text{H}}^2 \gamma_{\text{C}} \gamma_{\text{N}}}{r_{\text{NH}}^3 r_{\text{CH}}^3} \frac{(3 \cos^2 \theta^{\text{CHNH}} - 1)}{2} \frac{2S^2 \tau_{\text{c}}}{5} \quad (17)$$

where r_{CH} and r_{NH} are the $\text{C}^\alpha\text{-H}^\alpha$ and N-H^N bond distances and $\theta_{\text{CH,NH}}$ is the angle subtended between the $\text{C}^\alpha\text{-H}^\alpha$ and N-H^N internuclear vectors, τ_{c} is the global rotational correlation time assuming isotropic overall tumbling and S is the generalized Lipari-Szabo order parameter.^{19,20} Assuming the peptide bond to be planar (see Figure 1), the angle $\theta_{\text{CH,NH}}$ is related to the backbone angle Ψ in the following way:

$$\theta_{\text{CH,NH}} = \cos^{-1}[0.163 + 0.819 \cos(\Psi - 120^\circ)] \quad (18)$$

Similarly, $R_{\text{C}'\text{C}^\alpha\text{H}^\alpha} \gg R_{\text{C}'\text{H}^\alpha\text{C}^\alpha}$, so $\Gamma_1' \approx R_{\text{C}'\text{C}^\alpha\text{H}^\alpha}$. In the slow tumbling limit one obtains

$$\Gamma_1' = \left(\frac{\mu_0 \hbar}{4\pi}\right)^2 \frac{\gamma_{\text{C}}^2 \gamma_{\text{H}}}{r_{\text{CH}}^3} \frac{2B_0}{3} F(\sigma_X, \sigma_Y, \sigma_Z) \frac{2S^2 \tau_{\text{c}}}{5} \quad (19)$$

where B_0 is the static magnetic field and $F(\sigma_X, \sigma_Y, \sigma_Z)$ is given by^{9,10,12}

$$F(\sigma_X, \sigma_Y, \sigma_Z) = 1/2[\sigma_X(3 \cos^2 \theta_X - 1) + \sigma_Y(3 \cos^2 \theta_Y - 1) + \sigma_Z(3 \cos^2 \theta_Z - 1)] \quad (20)$$

where σ_i ($i = X, Y, Z$) are the three principal components of the C' chemical shift tensor and θ_i ($i = X, Y, Z$) are the angles

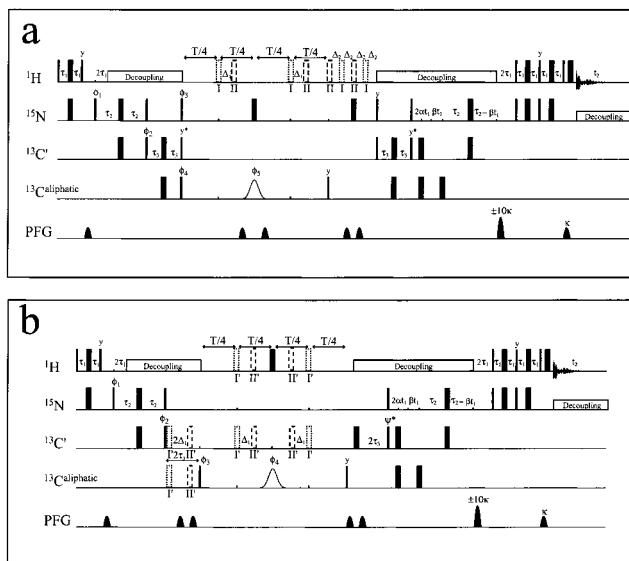


Figure 4. Pulse sequences employed for the measurement of cross-correlation rates (a) $R_{\text{C}^\alpha\text{H}^\alpha\text{NH}^\text{N}}$ and (b) $R_{\text{C}'\text{C}^\alpha\text{H}^\alpha}$. Narrow and wide rectangles indicate $\pi/2$ and π pulses. The $^{13}\text{C}^\alpha$ π pulse in the middle of the relaxation period T has a RE-BURP²⁴ profile (typically of 2.5 ms duration to cover 16 ppm at 100 MHz). The ^1H π pulse at $T/2$ in (b) is applied after the soft $^{13}\text{C}^\alpha$ pulse in order to allow refocusing of the scalar coupling (if they are applied simultaneously they interfere with each other). The fixed delays are set to $\tau_1 = 1/4J(\text{NH}^\text{N})$, $\tau_2 = 1/4J(\text{C}'\text{C}^\alpha)$, $\Delta_1 = 1/8J(\text{C}^\alpha\text{H}^\alpha)$ and $\Delta_2 = \{1/8J(\text{NH}^\text{N}) - 1/8J(\text{C}^\alpha\text{H}^\alpha)\}$. The relaxation period T must be larger than $1/2J(\text{C}^\alpha\text{H}^\alpha)$ so that the pulses can be shifted over a suitable range in experiments I and II'. The ^{15}N magnetization evolves freely during $2\alpha_1$, then in the manner of a constant time experiment during the period where the $J_{\text{NC}'}$ scalar coupling is refocused. The constant α can be chosen to obtain the desired resolution in the ^{15}N chemical shift domain. Detection is achieved using echo-antiecho gradient selection to enhance sensitivity.²⁵ Unless specified otherwise, all pulses are applied along the x -axis. Phase corrections for Bloch-Siegert shifts must be optimized for all pulses marked with stars. In experiments I and II the phase cycle is $\Phi_1 = (x), (-x); \Phi_2 = 2(x), 2(-x); \Phi_3 = 4(y), 4(-y); \Phi_4 = 8(y), 8(-y); \Phi_5 = 16(x), 16(y), 16(-x), 16(-y)$. In experiments I' and II' the phase cycle is $\Phi_1 = (x), (-x); \Phi_2 = 2(y), 2(-y); \Phi_3 = 4(y), 4(-y); \Phi_4 = 8(x), 8(y), 8(-x), 8(-y)$. For experiments I' and II', the phase Ψ must be y and x , respectively. Decoupling of the proton and nitrogen channels can be achieved with WALTZ-16²⁶ and GARP.²⁷

subtended between the internuclear $\text{C}^\alpha\text{-H}^\alpha$ vector and the three principal axes of the shift tensor. Except for glycine residues in proteins we may assume that the CSA tensor is oriented as shown in Figure 1 and the angles θ_i are related to the backbone Ψ angle in the following way:^{9,10,12}

$$\begin{aligned} \theta_X &= \cos^{-1}[-0.3095 + 0.3531 \cos(\Psi - 120^\circ)] \\ \theta_Y &= \cos^{-1}[-0.1250 - 0.8740 \cos(\Psi - 120^\circ)] \\ \theta_Z &= \cos^{-1}[-0.9426 \sin(\Psi - 120^\circ)] \end{aligned} \quad (21)$$

Results and Discussion

Experiments I and II To Measure $R_{\text{C}^\alpha\text{H}^\alpha\text{NH}^\text{N}}$. Figure 4a shows two sequences which make it possible to measure the signal amplitudes required for the ratio of eq 11b. First, the multiple quantum coherence $4N_x\text{C}^\alpha_x\text{C}'_z$ is excited.²¹ Hereafter, the scheme of Figure 3a is inserted. After the relaxation time T , either of the two terms $4N_x\text{C}^\alpha_x\text{C}'_z$ or $16N_y\text{C}^\alpha_y\text{C}'_z\text{H}^\alpha_z\text{H}^\text{N}_z$ need to be converted into an observable signal. In experiment I, we

(19) Lipari, G.; Szabo, A. *J. Am. Chem. Soc.* **1982**, *104*, 4546.

(20) Lipari, G.; Szabo, A. *J. Am. Chem. Soc.* **1982**, *104*, 4558.

(21) Bax, A.; Ikura, M. *J. Biomol. NMR* **1991**, *1*, 99.

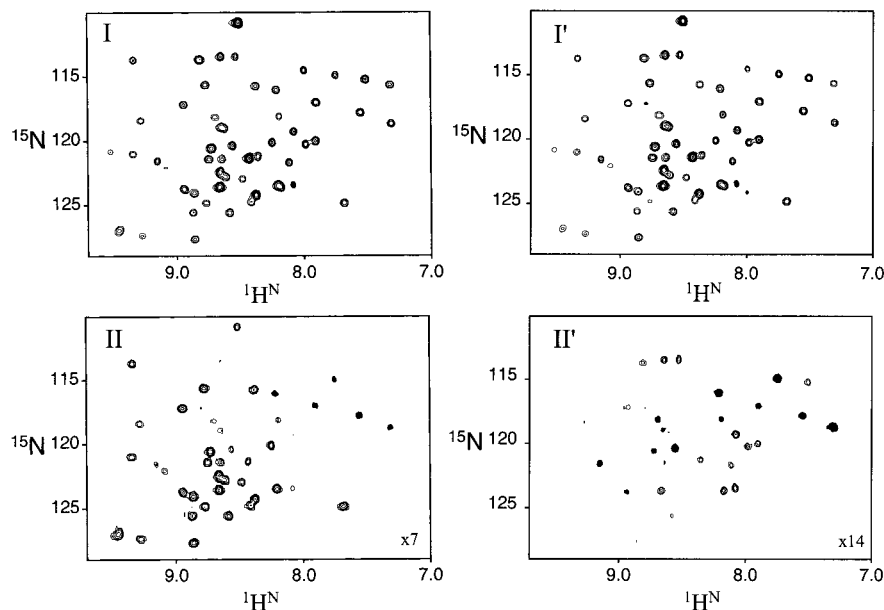


Figure 5. Experimental spectra of ^{15}N , ^{13}C -labeled human ubiquitin obtained with the sequences I, II, I', and II' of Figure 3 with a relaxation interval $T = 17$ ms. The ratios of the cross-peak amplitudes $a(\text{II})/a(\text{I})$ and $a(\text{II}')/a(\text{I}')$ give the rates $R_{C^{\alpha}\text{H}^{\alpha},\text{NH}^{\text{N}}}$ and $R_{C^{\alpha},C^{\alpha}\text{H}^{\alpha}}$, respectively. Negative cross-peaks are filled in black. The digital resolution in the ω_1 dimension is 11 Hz, and 128 scans were accumulated for each of the 148 t_1 points, resulting in a total experimental time of 7.5 h per experiment. The experiments have been carried out with a 1.5 mM sample of ^{15}N , ^{13}C -labeled human ubiquitin (VLI Research) in $\text{H}_2\text{O}:\text{D}_2\text{O} = 9:1$ buffered at pH 4.5 at 303 K with a Bruker 400 MHz Avance spectrometer equipped with a triple resonance TBO probe. All data-processing and peak-picking were carried out using the NMRpipe and NMRdraw software.²⁸

collect $4N_x C^{\alpha}_x C'_z$ directly, while in experiment II, $16N_y C^{\alpha}_y C'_z H^{\alpha}_z H^{\text{N}}_z$ is first converted into $4N_x C^{\alpha}_x C'_z$, by moving the two ^1H pulses by $\Delta_1 = 1/8J(C^{\alpha}\text{H}^{\alpha})$ during the T period. This generates an asymmetry of $4\Delta_1 = 1/2J(C^{\alpha}\text{H}^{\alpha})$ in the sequence which allows the scalar coupling $J(C^{\alpha}\text{H}^{\alpha})$ to convert $2C^{\alpha}_y H^{\alpha}_z$ into C^{α}_x . The $J(\text{NH}^{\text{N}})$ coupling acts not only during $4\Delta_1$ but also in an extra period of duration $4\Delta_2 = 1/2J(\text{NH}^{\text{N}}) - 1/2J(C^{\alpha}\text{H}^{\alpha})$ to convert $2N_y H^{\text{N}}_z$ into N_x . To have similar signal attenuation in the two experiments, a period of duration $4\Delta_2$ with the same number of pulses, but positioned so that evolution under scalar couplings is suppressed, is also inserted in experiment I (see Figure 4a). Note that $J(\text{NH}^{\text{N}})$ and $J(C^{\alpha}\text{H}^{\alpha})$ have opposite signs (because $\gamma_{\text{N}} < 0$) so that $16N_y C^{\alpha}_y C'_z H^{\alpha}_z H^{\text{N}}_z$ is converted into $-4N_x C^{\alpha}_x C'_z$, hence the minus sign in eq 11b. The π pulse at $T/2$ inverts only the C^{α} nuclei (but not the C^{β} or the C' nuclei), thus the time T does not need to be set to a multiple of $1/J(C^{\alpha}C^{\beta})$.¹⁰ Note that shifting pulses in experiment II relative to experiment I does not influence other relaxation properties (see Figure 3). At the end of both experiments I and II, the multiple-quantum term $4N_x C^{\alpha}_x C'_z$ is transferred back to the H^{N} proton. Both experiments include an evolution period to separate the signals according to the ^{15}N chemical shifts.¹¹ The intensity ratios of the cross-peaks observed in the two 2D spectra is given by eq 11b.

Experiments I' and II' To Measure $R_{C^{\alpha},C^{\alpha}\text{H}^{\alpha}}$. The pulse sequences of Figure 4b are designed to measure $R_{C^{\alpha},C^{\alpha}\text{H}^{\alpha}}$. A term $2C'_y N_z$ is first created through successive transfers and converted into a doubly antiphase coherence $4C^{\alpha}_z C'_x N_z$ during a delay $2\tau_3 = 1/2J(C^{\alpha}C')$. A semiselective $\pi/2$ pulse applied to the aliphatic carbons converts this into $4C^{\alpha}_x C'_x N_z$, as discussed elsewhere.^{10,21} The scheme of Figure 3b is then inserted to allow a partial conversion of $4C^{\alpha}_x C'_x N_z$ into $8C^{\alpha}_y C'_y N_z H^{\alpha}_z$ under cross-correlated CSA $\{^{13}\text{C}'\}/\text{DD}\{^{13}\text{C}^{\alpha}-^1\text{H}^{\alpha}\}$. In experiment I' and II', a band-selective π pulse inverts the $^{13}\text{C}^{\alpha}$ at $T/2$ without perturbing the $^{13}\text{C}^{\beta}$ carbons.⁹ In experiment II' the simultaneous ^1H and $^{13}\text{C}'$ π pulses are shifted by $\Delta_1 = 1/8J(C^{\alpha}\text{H}^{\alpha})$ toward the center of the evolution period in order to create an asymmetry of $4\Delta_1 = 1/2J(C^{\alpha}\text{H}^{\alpha})$ which leads to the conversion of the term

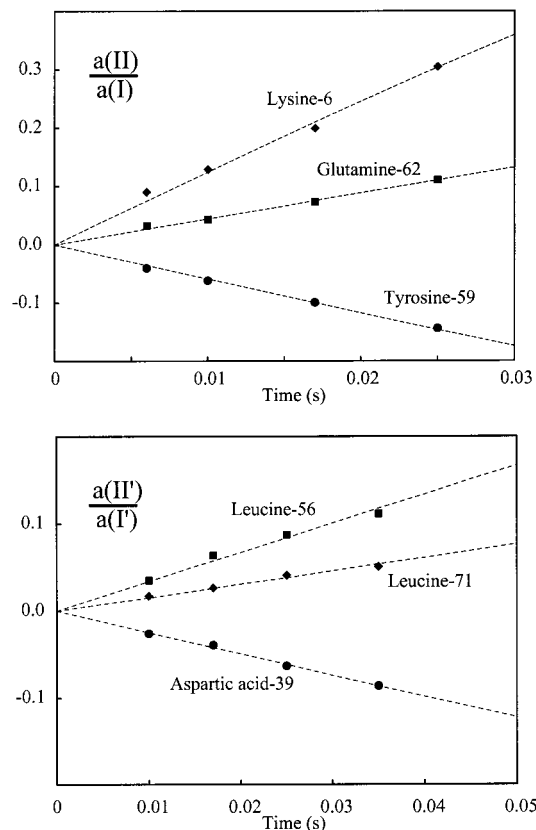


Figure 6. Examples of intensity ratios $a(\text{II})/a(\text{I})$ and $a(\text{II}')/a(\text{I}')$ as a function of the relaxation interval T . Two-spin coherences $C^{\alpha}_x(n)N_x(n+1)$ or $C^{\alpha}_x(n)C'_x(n)$ are identified by the name of the n th amino acid. The dashed lines are fits to eq 11b for $a(\text{II})/a(\text{I})$ and eq 16b for $a(\text{II}')/a(\text{I}')$.

$8C^{\alpha}_y C'_y N_z H^{\alpha}_z$ into $4C^{\alpha}_x C'_x N_z$. After a $\pi/2$ pulse on $^{13}\text{C}^{\alpha}$, the terms $4C^{\alpha}_z C'_x N_z$ and $4C^{\alpha}_z C'_y N_z$ are transformed during a second period of $2\tau_3 = 1/2J(C^{\alpha}C')$ into $2C'_y N_z$ or $2C'_x N_z$ in experiments I' or II', respectively. Thus, the $^{13}\text{C}'$ "read" pulse has to be shifted

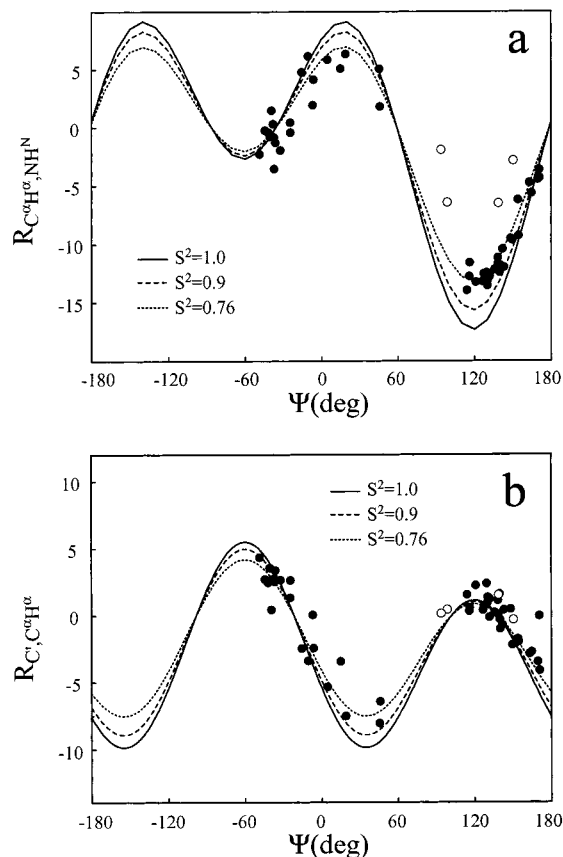


Figure 7. Experimental cross-correlation rates $R_{C^{\alpha}H^{\alpha},NH^N}$ and $R_{C',C^{\alpha}H^{\alpha}}$ plotted as a function of the backbone angle Ψ found for 53 well-resolved amino acids (except glycines) from the X-ray structure of ubiquitin. The curves represent the theoretical dependence derived from eqs 17 and 18 for $R_{C^{\alpha}H^{\alpha},NH^N}$ and from eqs 19–21 for $R_{C',C^{\alpha}H^{\alpha}}$. The correlation time was assumed to be 4 ns. The values of σ_X , σ_Y , and σ_Z (see Figure 1) were assumed to be 244, 178, and 90 ppm.²⁹ The three curves correspond to order parameters $S^2 = 1, 0.90,$ and 0.76 . The rates corresponding to the four residues in the C-terminal loop which have a small order parameters are indicated by open circles.

in phase by 90° in experiment II' relative to experiment I'. Evolution under $^{13}C'$ chemical shifts is suppressed in both experiments by applying a $^{13}C'$ π pulse right after the relaxation period T . In experiment II' two simultaneous π pulses on $^{13}C'$ and $^{13}C^{\alpha}$ are applied at $2\Delta_1 = 1/4J(C^{\alpha}H^{\alpha})$ after the first $\pi/2$ $^{13}C'$ pulse, while in the experiment I' these two pulses are applied immediately after the $\pi/2$ $^{13}C'$ pulse. Again, shifting the pulses does not influence the relaxation properties (see Figure 3). Like in the experiments I and II, we record two complementary 2D spectra and determine the ratio of the intensities according to eq 16b.

Applications to $^{15}N,^{13}C$ -Labeled Human Ubiquitin. Figure 5 shows parts of 2D spectra obtained with the four experiments described in Figure 4. Experiments I and II were performed with relaxation delays $T = 6, 10, 17,$ and 25 ms, while I' and II' were performed with $T = 10, 17, 25$ and 35 ms. In Figure 6, the ratios of the signal amplitudes a_{II}/a_I and $a_{II'}/a_{I'}$ are plotted for some selected residues as function of T and fitted to eqs 11b and 16b, respectively. The fits were performed using the subroutines of the ODRPACK library.²²

In Figure 7 the values of $R_{C^{\alpha}H^{\alpha},NH^N}$ and $R_{C',C^{\alpha}H^{\alpha}}$ obtained from these fits are plotted against the Ψ angles observed in the X-ray

(22) Boggs, P. T.; Byrd, R. H.; Rogers, T. E.; Schnabel, R. B. *User's Reference Guide for ODRPACK 2.01—Software for Weighted Orthogonal Distance Regression*; NIST IR4834; U.S. Government Printing Office: Washington, DC, 1992.

structure.²³ The curves in Figure 7 represent the rates predicted from eqs 17–21 calculated for three different values of the order parameter S^2 . Except for the terminal residues, most residues in ubiquitin have S^2 values which lie between 0.76 and 0.9.¹

Conclusion

In this paper, we have presented a compact theoretical treatment of the effects of cross-correlated relaxation mechanisms on the relaxation of two-spin coherences involving various nuclei in $^{15}N,^{13}C$ -labeled proteins. We have presented improved experiments to measure cross-correlation between the dipolar $^{13}C^{\alpha}-^1H^{\alpha}$ and $^{15}N-^1HN$ interactions on two-spin coherences involving the $^{13}C^{\alpha}$ nucleus of the i th residue of a protein and the ^{15}N nucleus of the neighboring residue ($i + 1$). We have also presented experiments to measure cross-correlation between the $^{13}C'$ (carbonyl) CSA and the dipolar $^{13}C^{\alpha}-^1H^{\alpha}$ coupling on the relaxation of two-spin coherence involving the $^{13}C'$ and $^{13}C^{\alpha}$ nuclei of the i th residue of a protein. These methods have been applied to $^{15}N,^{13}C$ -labeled human ubiquitin to extract the relevant cross-correlation rates, which we have demonstrated to be related to the backbone angle Ψ in proteins.

Appendix

A. Perturbation Expansion of the Relaxation Matrix. The effect of the off-diagonal elements of eq 5 on the dynamics of the spin system can be determined by using perturbation theory.¹⁸ We illustrate this by considering the submatrix \mathbf{R}^{++} given in eq 5a. \mathbf{R}^{++} may be split into two matrixes, \mathbf{R}_D^{++} and \mathbf{R}_{ND}^{++} :

$$\mathbf{R}_D^{++} = \begin{pmatrix} i\pi J_{++} + R_{av} + R_{DQ\alpha\alpha} & 0 & 0 & 0 \\ 0 & i\pi J_{+-} + R_{av} + R_{DQ\alpha\beta} & 0 & 0 \\ 0 & 0 & -i\pi J_{+-} + R_{av} + R_{DQ\beta\alpha} & 0 \\ 0 & 0 & 0 & -i\pi J_{++} + R_{av} + R_{DQ\beta\beta} \end{pmatrix} \quad (A-1)$$

It is to be noted that \mathbf{R}_{ND}^{++} is Hermitian even though \mathbf{R}^{++} is

$$\mathbf{R}_{ND}^{++} = \begin{pmatrix} 0 & \frac{R_{ii} + R_{ai} - R_{ia} - R_{aa}}{4} & \frac{R_{ii} - R_{ai} + R_{ia} - R_{aa}}{4} & \frac{R_{ii} - R_{ai} - R_{ia} + R_{aa}}{4} \\ \frac{R_{ii} + R_{ai} - R_{ia} - R_{aa}}{4} & 0 & \frac{R_{ii} - R_{ai} - R_{ia} + R_{aa}}{4} & \frac{R_{ii} - R_{ai} + R_{ia} - R_{aa}}{4} \\ \frac{R_{ii} - R_{ai} + R_{ia} - R_{aa}}{4} & \frac{R_{ii} - R_{ai} - R_{ia} + R_{aa}}{4} & 0 & \frac{R_{ii} + R_{ai} - R_{ia} - R_{aa}}{4} \\ \frac{R_{ii} - R_{ai} - R_{ia} + R_{aa}}{4} & \frac{R_{ii} + R_{ai} - R_{ia} - R_{aa}}{4} & \frac{R_{ii} + R_{ai} - R_{ia} - R_{aa}}{4} & 0 \end{pmatrix} \quad (A-2)$$

non-Hermitian. \mathbf{R}_{ND}^{++} can be treated as a perturbation on \mathbf{R}_D^{++} . The first-order corrections to the matrix elements of \mathbf{R}_D^{++} vanish. The second-order corrections are given by

$$(R^{++})_{ii}^{(2)} = \sum_{i \neq j} \frac{(R_{ND}^{++})_{ij} (R_{ND}^{++})_{ji}}{(R_D^{++})_{ii} - (R_D^{++})_{jj}} = \sum_{i \neq j} \frac{(R_{ND}^{++})_{ij}^2}{(R_D^{++})_{ii} - (R_D^{++})_{jj}} \quad (A-3)$$

where we have utilized the Hermitian character of \mathbf{R}_{ND}^{++} . The

(23) Vijay-Kumar, S.; Bugg, C. E.; Cook, C. J. *J. Mol. Biol.* **1987**, *194*, 531.

(24) Geen, H.; Freeman, R. *J. Magn. Reson.* **1991**, *93*, 93.

(25) Palmer, A., III; Cavanagh, J.; Wright, P. E.; Rance, M. *J. Magn. Reson.* **1991**, *93*, 151.

(26) Shaka, A. J.; Keeler, J.; Frenkiel, T.; Freeman, R. *J. Magn. Reson.* **1983**, *52*, 335.

(27) Shaka, A. J.; Barker, P. B.; Freeman, R. *J. Magn. Reson.* **1985**, *64*, 547.

(28) Delaglio, F.; Grzesiek, S.; Vuister, G. W.; Zhu, G.; Pfeifer, J.; Bax, A. *J. Biomol. NMR* **1995**, *6*, 277.

(29) Teng, Q.; Iqbal, M.; Cross, T. *J. Am. Chem. Soc.* **1992**, *114*, 5312.

second-order corrections obtained from eq A-3 are complex and comprise both real and imaginary parts. One can estimate the second-order correction to the eigenvalues by assuming that $R_{DQ\alpha\alpha} - R_{DQ\alpha\beta} \approx R_{DQ\alpha\alpha} - R_{DQ\beta\alpha} \approx R_{C^{\alpha}H^{\alpha},NH^N}$, $R_{ia} \approx R_{ai} \approx R_{ii} + R_1^H$, and $R_{aa} \approx R_{ia} + R_1^H \approx R_{ii} + 2R_1^H$, where R_1^H is the contribution to the T_1 of $^1H^N$ (or $^1H^{\alpha}$) due to homonuclear dipolar interactions with other 1H 's. Assuming a $R_{C^{\alpha}H^{\alpha},NH^N}$ of 15.0 s^{-1} (which is an upper limit in the present case) and a R_1^H of 6.4 s^{-1} , we obtain a value of about 0.01 s^{-1} for the real part of the correction, i.e., a negligible adjustment of the decay rates of the coherences. Similarly, the imaginary part (which gives rise to frequency shifts of the components of the doublet-of-doublets) corresponds to about 0.08 Hz . These corrections are evidently very small and may be neglected in the present case.

A special case arises when $J_{+-} = 0$, which may be the case when one studies the effects of cross-correlation between two $^1H-^{13}C$ dipolar interactions, say in the case of $^{13}C^{\alpha}-^1H^{\alpha}$, $^{13}C^{\beta}-^1H^{\beta}$ pairs. This condition corresponds to the overlap of the two central lines of the doublet-of-doublets in the zero- and double-quantum spectra. In this case, the above form of perturbation theory can no longer be used since $(R_D^{++})_{22} \approx (R_D^{++})_{33}$ (due to the fact that $R_{DQ\alpha\beta} \approx R_{DQ\beta\alpha}$). In this case, we can remove the degeneracy (to first order) by forming linear combinations of the spin-states corresponding to these rates. The resulting nondegenerate states are given by

$$b_2' = a_+^{(2)} 2C_+^{\alpha} C_+^{\beta} + H_{\alpha}^{\alpha} C_{\beta}^{\beta} + a_+^{(3)} 2C_+^{\alpha} C_+^{\beta} + H_{\beta}^{\alpha} C_{\alpha}^{\beta} \quad (A-4)$$

$$b_3' = a_-^{(2)} 2C_+^{\alpha} C_+^{\beta} + H_{\alpha}^{\alpha} C_{\beta}^{\beta} + a_-^{(3)} 2C_+^{\alpha} C_+^{\beta} + H_{\beta}^{\alpha} C_{\alpha}^{\beta} \quad (A-4)$$

The corresponding diagonal elements of the altered \mathbf{R}^{++} matrix (correct to first order) are given by

$$R_{22}^{++\nu} = R_{av} + R_+ \quad (A-5)$$

$$R_{33}^{++\nu} = R_{av} + R_- \quad (A-5)$$

$$R_{\pm} = \frac{1}{2} \{ [R_{DQ\alpha\beta} + R_{DQ\beta\alpha}] \pm [(R_{DQ\alpha\beta} - R_{DQ\beta\alpha})^2 + 4R_{\Delta}^2]^{1/2} \} \quad (A-6)$$

where

$$R_{\Delta} = \frac{1}{4} (R_{ii} - R_{ai} - R_{ia} + R_{aa}) \quad (A-7)$$

The mixing coefficients $a_{\pm}^{(2)}$ and $a_{\pm}^{(3)}$ in eq A-4 are given by

$$a_{\pm}^{(2)} = \frac{R_{DQ\alpha\beta} - R_{\pm}}{\sqrt{(R_{DQ\alpha\beta} - R_{\pm})^2 + R_{\Delta}^2}} \quad (A-8)$$

$$a_{\pm}^{(3)} = \frac{-R_{\Delta}}{\sqrt{(R_{DQ\alpha\beta} - R_{\pm})^2 + R_{\Delta}^2}} \quad (A-8)$$

It is evident that the coherences are mixed if their precession frequencies are nearly equal. Thus, to first order, the coupled differential equations governing the evolution of \mathbf{b}^{++} in eq 3 split up into one subspace of dimensions 2 and two of dimension 1.

B. Cross-Correlation Rates. In the slow-tumbling limit, the relaxation rate due to cross-correlation of the fluctuations of two dipole-dipole interactions is given by

$$R_{ij,kl} = \left(\frac{\mu_0 \hbar}{4\pi} \right)^2 \frac{\gamma_i \gamma_j \gamma_k \gamma_l}{r_{ij}^3 r_{kl}^3} \left(\frac{3 \cos^2 \theta_{ij,kl} - 1}{2} \right) \frac{2S^2 \tau_c}{5} \quad (B-1)$$

where r_{ij} and r_{kl} are the internuclear distances and $\theta_{ij,kl}$ is the angle subtended between the two internuclear vectors. The other symbols have their usual meaning.

The relaxation rate due to cross-correlation of the fluctuations of a dipole-dipole interaction and a chemical shift anisotropy in the slow tumbling limit is given by

$$R_{ijk} = \left(\frac{\mu_0 \hbar}{4\pi} \right) \frac{\gamma_i \gamma_j \gamma_k}{r_{jk}^3} \frac{2B_0}{3} \sum_{\xi} \frac{\sigma_{\xi}^i (3 \cos^2 \theta_{\xi}^i - 1)}{2} \frac{2S^2 \tau_c}{5} \quad (B-2)$$

with $\xi = x, y, z$ where σ_{ξ}^i is the ξ th principal component of the CSA of spin i and θ_{ξ}^i is the angle subtended between the ξ th principal axis of the CSA tensor and the internuclear vector.

The general case of cross-correlation between the CSA's of two nuclei i and j , where both nuclei have chemical shift tensors which are not axially symmetric, leads to rather cumbersome expressions. Some simplification is obtained when one of the chemical shift tensors (say for nucleus i) is axially symmetric. In this case, the rate is given by

$$R_{ij} = \gamma_i \gamma_j \frac{2B_0 \Delta \sigma^j}{9} \sum_{\xi} \frac{\sigma_{\xi}^i (3 \cos^2 \theta_{\xi}^j - 1)}{2} \frac{2S^2 \tau_c}{5} \quad (B-3)$$

where $\Delta \sigma^j$ is the CSA of nucleus i and $\xi = x, y, z$ where σ_{ξ}^j is the ξ th principal component of the CSA of spin j and θ_{ξ}^j is the angle subtended between the ξ th principal axis of the CSA with the unique axis of the CSA tensor of nucleus i .

Supporting Information Available: Table giving $R_{C^{\alpha}H^{\alpha},NH^N}$ and $R_{C^{\alpha}H^{\alpha}}$ values in ubiquitin (PDF). This material is available free of charge via the Internet at <http://pubs.acs.org>.

JA984390P